Laser Fusion Hydrodynamics Calculations

G.A. Moses

February 1977

UWFDM-195

Nuclear Science and Engineering 64, 49 (1977).

FUSION TECHNOLOGY INSTITUTE

UNIVERSITY OF WISCONSIN

MADISON WISCONSIN

Laser Fusion Hydrodynamics Calculations

G.A. Moses

Fusion Technology Institute
University of Wisconsin
1500 Engineering Drive
Madison, WI 53706

http://fti.neep.wisc.edu

February 1977

UWFDM-195

Nuclear Science and Engineering 64, 49 (1977).

Laser Fusion Hydrodynamics Calculations

by

Gregory A. Moses

UWFDM-195

Invited Paper:

Mathematics and Computation Division
Topical Meeting - American Nuclear Society
March 28-30, 1977
Tucson, Arizona

Published In Nuclear Science and Engineering 64 (1977) 49-63.

I. Introduction

The successful development of the laser driven fusion concept of CTR[1-3] depends upon understanding many time dependent coupled nonlinear processes typically represented by the plasma hydrodynamics equations and various other transport (Boltzmann or Fokker-Planck) equations. It is the carefully programmed coupling of laser light into the underdense plasma, conversion of the energy to an electron thermal conduction wave, and finally the conversion of the thermal electron energy to hydrodynamic motion that sets the stage for the spherical implosion process that ultimately leads to very high adiabatic compressions, Fig. 1. As the spherical shock waves converge to the pellet center with a velocity in excess of 3×10^7 cm/sec, they shock heat the central region of the compressed pellet to 4-10 keV and thermonuclear burning results. This burning self-heats the central region to over 20 keV and a supersonic burn wave propagates outward from the pellet center heating the surrounding, cold, adiabatically compressed plasma by redeposition of charged particle DT and DD reaction products. As the surrounding plasma heats, it begins to burn, thus driving the burn wave, Fig. 2.[4]

The success of this scenario depends sensitively upon many details of the implosion and energy transport process. During the implosion process, the plasma can be divided into three spatial regions as shown in Fig. 1. The outermost region is bordered by the outer edge of the plasma and the critical density surface where the electron plasma frequency is equal to the laser light frequency, $10^{21} cm^{-3}$ for 1.06 μm radiation and $10^{19} cm^{-3}$ for 10.6 μm radiation. It is in this region that laser light is absorbed or reflected from the plasma with most of the action taking place near the critical density surface. The laser light absorption is typically characterized

as classical (or inverse bremsstrahlung) absorption and anomalous absorption. Anomalous absorption can result from many different wave-wave couplings, with the most popular being resonant absorption, a coupling of the laser electric field with electron plasma waves.[5] This requires non-normal incidence of the laser light on the electron density gradient in this outer, or corona region, near the critical density surface. Since this electron density gradient also refracts the laser light, there will be an optimum angle at which resonant absorption is maximized, Fig. 3.[6] In actual practice, this resonant absorption process cannot be self-consistently determined within a laser fusion hydrodynamics calculation, for the time and spatial scales are far too small. Instead, the results of numerical plasma simulations and experiments are used to provide a recipe for determining the amount of energy absorbed through resonant absorption. The resonant absorption process also leaves its energy with very few, very energetic electrons.[7] These so called suprathermal electrons may be 10 to 100 times hotter than the thermal background plasma and consequently possess mean-free-paths that are very long in comparison with the gradients in the thermal plasma. In the corona region, these suprathermal electrons are presumed to give rise to fast ions that are observed in laser-plasma experiments.[8] Those hot electrons streaming inward from the critical density surface can stream ahead of the ablation front and preheat the compressing pellet core, Fig. 1. This will result in a degradation of the implosion process.[9] It is therefore very important to correctly treat these suprathermal electrons, both with regard to their origin and their transport, if a hydrodynamics code is to properly model the behavior of current experiments or predict the ultimate success of laser fusion.

In addition to this non-hydrodynamic coupling of laser energy into the plasma electrons, there is also a contribution to the hydrodynamic pressure due to the presence of the laser radiation near the critical density. This so called ponderomotive force, due to the intense radiation field, can significantly alter the electron density gradient profile near the critical density surface and thus can affect both the classical and resonant absorption processes.[8] This makes even more difficult the job of properly modelling the coupling of laser light into the plasma. To date no laser fusion hydrodynamics code can consistently predict the amount of laser energy deposited into the plasma. Typically the amount of energy deposited is determined by a prescription that comes from the particular experiment being modelled, and the remainder of the simulation is performed under this assumption.

The second region of interest is bordered by the critical density surface on the outside and the ablation front on the inside. This region has a fluid velocity in the positive (outward) direction, however, the dominant energy flow is inward via the thermal electron conduction process and suprathermal electron streaming. Thus it is the transport of energy that is of most importance in this region, underscoring the fact that laser fusion calculations should not be considered as hydrodynamic calculations in the classical sense. Generally, a hydrodynamics problem is one where mass flow is the dominant process. In this middle region however, the energy flow is an equally dominant process with thermal conduction and transport of non-thermal energy no longer representing a first order effect. It will be seen later that for this reason the use of standard procedures for computing transport coefficients will lead to erroneous results in hydrodynamics calculations and

ad-hoc fix-ups must be made to the equations to insure plausible results.

The sensitivity of the implosion process to uncertainties in the electron thermal conduction process are displayed in Fig. 4 where the thermal conductivity was scaled up and down from its nominal value. The maximum compression of the pellet core was reduced by over an order of magnitude for changes in K_e within the uncertainty of its correct value. Important reductions of K_e can result from both plasma instabilities and locally intense self-generated magnetic fields. Ion acoustic instabilities[10] are the result of the strong electron stream representing the thermal conduction and the counter streaming cold electron return current that is trying to maintain charge neutrality. These instabilities can lead to an increase in the electron-ion collision frequency and thus will reduce the thermal conduction. Again, these transport coefficient computations cannot be done in a self-consistent fashion within a hydrodynamic calculation but must be approximated by using a prescription such as ratios of electron and ion temperatures and the magnitude of the electron heat flux. Self-generated magnetic fields can result from thermo-electric currents that are produced in an inhomogeneous plasma.[11] One typical situation is non-parallel density and temperature gradients, $\nabla n \times \nabla T$, that are the result of non-uniform laser illumination and/or the development of two-dimensional flow during the implosion process. Two-dimensional flow can result from a non-symmetric target configuration, such as a balloon disc, or from the development of fluid instabilities during a symmetric implosion. In either case, the thermal transport coefficient transverse to the magnetic field lines is reduced by the factor $(1 + \omega^2\tau^2)^{-1}$ where ω is the electron-cyclotron frequency and τ is the electron-ion collision frequency.[12]

The point here is that a two-dimensional hydrodynamic treatment is necessary to predict this important effect, even for a presumably symmetric implosion. This is of great significance because two-dimensional calculations are extremely expensive and the accurate treatment of the transport processes that are important in addition to the hydrodynamics are prohibitively expensive in two-dimensions.

The third region of interest is that part of the pellet within the ablation surface. In this dense, cold plasma, hydrodynamics is presumably an accurate model, however care must be taken to properly evaluate the associated plasma equations of state. At high compressions, the cold electrons behave as Fermions and their properties must be treated accordingly. The other hydrodynamic effect of interest is the fluid instability. Conditions at the ablation front can correspond to the Rayleigh-Taylor instability conditions and growth rates can be fast enough to destroy the isentropic implosion necessary to the success of laser fusion. This again necessitates the use of more than a one-dimensional treatment of the hydrodynamic flow. Perturbation techniques as well as fully two-dimensional calculations have been used to study this problem.[13-16]

For all three of these regions, radiation emission, absorption and transport must also be considered. High energy photons created in the laser absorption region can stream inward to preheat the pellet core just as the suprathermal electrons. More importantly, in the current experiments, radiation is one of the principal diagnostic tools. The spectrum is used to determine the electron temperature, the suprathermal electron temperature and the number of suprathermal electrons.[17] The spatial distribution of X-rays provides information regarding the compression of glass micro balloon pellets

and X-ray line emission has been used to diagnose the presence of suprathermal electron preheat of the compressed DT fuel.[18]

In addition to the three spatial regions discussed, there is a final stage of the laser fusion process that involves the burning of the compressed core. Upon ignition of the central hot "microcore" the burn process progresses much more rapidly than the implosion process itself. It can in fact be decoupled from the implosion process for a non-marginal burn, that is a burn that results in pellet gains near 100. This process again involves the transport of non-thermal particles, the charged particle fusion reaction products. These particles will slow down in the dense pellet core giving up their energy to bootstrap heat the core to optimum burn temperatures. In current laser fusion experiments, a negligible amount of charged particle energy is redeposited in the DT fuel, however the escaping particles are used as a diagnostic to determine the temperature of the burning fuel. In this case the charged particle transport must be done to predict the amount of energy loss and spectrum broadening that results from interactions with the surrounding glass shell, so that experimental results can be translated into DT ion temperatures.

The preceeding discussion has been an attempt to very briefly summarize the laser fusion problem and to highlight some of the more important physics that must be considered when modelling laser fusion plasmas. It was meant to show that classical hydrodynamics in itself is not nearly enough to model these plasmas and this directly translates into increased computing costs. The actual solution of the hydrodynamics equations represents only a small fraction of the computing cost. Complicated prescriptions for transport coefficients must be computed many times for almost all coefficients are non-linear and/or time dependent. Time dependent and energy dependent transport

calculations must be done and these are considerably more time consuming than the hydrodynamics equations because energy is typically represented in a multigroup structure. Due to the strong coupling between the energy, space, and time variables associated with charged particle slowing down, as many as 100 energy groups are needed to treat the transport problem.

In part II of this paper the numerical solution of the hydrodynamics equations will be discussed and in part III the general particle transport problem as it relates to laser fusion calculations will be discussed with a description of flux-limited diffusion theory and time dependent particle tracking. Any discussion of transport in laser fusion codes should include flux limited diffusion for this is the general transport method used in the most highly developed code to date, LASNEX. Time dependent particle tracking is a method that yields surprisingly good results for a particular kind of transport, non-thermal charged particle fusion reaction products.

II. Plasma Hydrodynamics

Almost all laser fusion plasma hydrodynamics codes use the two temperature-one fluid plasma model. In this model the electrons and ions are assumed to flow as one fluid implying no charge separation but each species maintains its own Maxwellian temperature due to the weak energy coupling between the two populations. Radiation can be included as either a third temperature equation, assuming a local Planckian distribution, or as an energy dependent treatment of the photon distribution function. Only the electrons and ions will be treated here because most typically the radiation is treated in an energy dependent fashion. In Lagrangian coordinates, where the finite difference mesh is embedded in the moving fluid, the hydrodynamic equations take the form

$$\frac{\partial \underline{u}(\underline{r},t)}{\partial t} = \frac{-1}{\rho(\underline{r},t)} \nabla(P(\underline{r},t) + q(\underline{r},t)) \tag{1}$$

$$\rho\, C_{ve} \frac{\partial T_e}{\partial t} = \nabla \cdot K_e \nabla T_e - P_e(\nabla \cdot \underline{u}) - \omega_{ei}(T_e - T_i) \tag{2}$$

$$- P_{eT}\dot{V}\, T_e + S_e$$

$$\rho\, C_{vi} \frac{\partial T_i}{\partial t} = \nabla \cdot K_i \nabla T_i - (P_i + q)(\nabla \cdot \underline{u}) + \omega_{ei}(T_e - T_i) \tag{3}$$

$$- P_{iT}\dot{V}\, T_i + S_i$$

where the terms are as follows:

$\underline{u}(\underline{r},t)$	fluid velocity
$\rho(\underline{r},t)$	plasma mass density
$P(\underline{r},t)$	plasma pressure
$q(\underline{r},t)$	Von Neumann artificial viscosity
$C_{ve}(\underline{r},t)$	electron specific heat at constant volume
$T_e(\underline{r},t)$	electron temperature
$K_e(\underline{r},t)$	electron thermal conductivity
$P_e(\underline{r},t)$	electron pressure
$\omega_{ei}(\underline{r},t)$	electron-ion energy coupling coefficient
$P_{eT}(\underline{r},t)$	temperature derivative of electron pressure
$\dot{V}(\underline{r},t)$	time derivative of specific volume
$S_e(r,t)$	electron energy source term
$C_{vi}(\underline{r},t)$	ion specific heat at constant volume
$T_i(\underline{r},t)$	ion temperature
$K_i(\underline{r},t)$	ion thermal conductivity
$P_i(\underline{r},t)$	ion pressure
$P_{iT}(\underline{r},t)$	temperature derivative of ion pressure
$S_i(\underline{r},t)$	ion energy source term.

These equations are both coupled and very nonlinear for $K_e \sim T_e^{5/2}$, $\omega_{ei} \sim T_e^{-3/2}$, etc.[19] They are usually solved using standard finite difference techniques.[20] Eqn. 1 is hyperbolic and has a characteristic propagation speed. It also will admit discontinuous solutions (shocks) that are a nightmare for general finite difference schemes. Because of these properties, this equation is usually solved using an explicit differencing technique:

$$\frac{\underline{u}^{n+1/2} - \underline{u}^{n-1/2}}{\Delta t^n} = -\frac{1}{\rho^n} \nabla(P^n + q^{n-1/2}) \tag{4}$$

where

$$\begin{aligned} q(\underline{r})^{n-1/2} &= q_{vn} && \text{for } \dot{V} < 0 \quad \text{(compression)} \\ q(\underline{r})^{n-1/2} &= 0 && \text{for } \dot{V} > 0 \quad \text{(expansion)} . \end{aligned} \tag{5}$$

The artificial viscosity is chosen in such a way that it dissipates energy in a shock to a few surrounding finite difference zones while preserving the Hugoniot relations across the shock.[21] This preserves the essential features of the shock while reducing the gradients across the shock to values that allow the time step to remain at reasonably large values. The spatial differencing has not been specified here for it will vary depending on whether the equation is solved in one or two dimensions. This equation requires a stability condition given by the Courant condition

$$\frac{C_s \, \Delta t}{\Delta X} < 1 \tag{6}$$

where C_s is the sound speed in the plasma. This condition of course says that a disturbance cannot be allowed to propagate across a finite difference zone in less than one time step.

The coupled temperature equations are parabolic, which should imply that they have an infinite propagation speed, however, due to the nonlinear thermal conductivity, they exhibit a behavior similar to that of a wave equation and in fact do have a finite propagation speed.[22] Nevertheless they are typically solved using an implicit differencing technique since their characteristic time scale is usually much less than the equation of motion, hence an explicit scheme would impose a much stricter time step constraint. They need not be solved simultaneously for their coupling is weak. The finite difference equations for each equation are of the form

$$\frac{T^{n+1} - T^n}{\Delta t^{n+1/2}} = \nabla \cdot K^n \nabla(\theta T^n + (1 - \theta)T^{n+1}) + \ldots \quad (7)$$

where again the specific spatial differencing has not been included. The parameter, θ, is taken as 1/2 for if the equations were linear (which they are not) and the Δt's and ΔX's were equal (which they are not) this value would give a second order accurate differencing scheme. In light of the non-linearities and the non-constant time and space steps, this can only be considered as trying to make the best of a bad situation. The nonlinear thermal conductivity has been shown with an explicit evaluation

$$K^n = K(T^n(\underline{r})) \quad (8)$$

in Eqn. 7 which is about the best that can be hoped for in a two-dimensional calculation. In a one-dimensional calculation, several other possibilities exist. Past temperatures at each mesh point can be saved and used to extrapolate ahead in time to evaluate K at n + 1/2,

$$\tilde{K}^{n+1/2} = K(\tilde{T}^{n+1/2}); \quad \tilde{T}^{n+1/2} = F(T^{n-2}, T^{n-1}, T^n), \quad (9)$$

or the temperature equations can be iterated by re-evaluating the nonlinear coefficients until the temperatures converge point-wise. Each of these methods has drawbacks even in one dimension however. Experience has shown that neither of them is as stable as the single explicit evaluation method and often they require more stringent conditions on the time step than the explicit evaluation. Furthermore, an "uninteresting" part of the plasma is usually the source of the smaller time step. In laser fusion calculations, the plasma electrons usually increase in temperature due to thermal conduction from a source of heat. This will be a stable process for these two schemes, however when electrons decrease in temperature, it is often because of an expansion of the plasma. The strong thermal conduction continually "feeds" these loss zones and an instability results.

For linear diffusion equations, the Crank-Nicholson ($\theta = 1/2$) differencing scheme will insure unconditional stability, however, this is not the case for the nonlinear equations where no rigorous estimate of the stability condition can be made. Experience has shown that a time step constrained to insure

$$\text{Max}[\Delta T/T] < 1/4 \qquad (10)$$

will usually provide stable solutions, however values as small as 1/10 have been necessary for some calculations and quite often it is this ad-hoc stability condition that sets the time step in the hydrodynamics calculation rather than the Courant condition.

In addition to these stability and accuracy problems, the hydrodynamics equations can suffer from the Lagrangian zoning. In one dimension, this presents

no problem, however, in two dimensions, it becomes a very significant problem. Since the mesh is embedded in the fluid, it distorts as the fluid motion evolves. This may not be a problem in two dimensions if the motion is well behaved, however, very often shear flows can develop and this is troublesome. Vortices also cannot be handled by Lagrangian coordinates. Fig. 5 demonstrates the problem with a very simple example of a strong force pushing diagonally on the corner of a quadrilateral zone. If the other mesh points of the zone remain fixed, then the zone develops a concave boundary and becomes a "banana zone." The temperature equations are usually solved in two-dimensions by making two "sweeps" through the mesh, one along the k-index lines and then along the l-index lines while holding the diffusion in the respective transverse direction fixed during each sweep, Fig. 6a. The problems of a banana zone become clear when the sweep path through the zone is indicated as in Fig. 5. Such badly distorted zones also demand very small time steps in order to maintain stability.

Many different "fix ups" have been devised to minimize or correct this zone distortion problem. A more sophisticated generalization of the artificial viscosity can be added to the code that will attempt to "discourage" zones from distorting while still maintaining the conservation properties of the fluid. When shear flow can be identified a priori the use of "slide lines" may be useful. Here, specified k or l lines are allowed to decouple as shown in Fig. 6b and slide against one another. This idea is conceptually simple but in practice is an extremely complex bookkeeping task to implement. A somewhat different approach involves stopping the calculation once zones have distorted sufficiently and rezoning the problem before continuing.

This is commonly done with most large two-dimensional codes and sophisticated computer graphics programs have been developed to allow the user to automatically re-position mesh points with a light pen. Here again the attempt is to maintain the conservation laws. Another method of computation known as mixed Eulerian-Lagrangian can also alleviate the zone distortion problem somewhat.

With all of these drawbacks there must be some very good reasons for using Lagrangian coordinates. They have the property that the mass of fluid that originally falls within the borders of a zone remains within that zone throughout the calculation. This mass is in fact used as an independent variable rather than $\underline{r}$ so equal mass zoning is usually desired. This is very important when materials with very different properties are adjacent to one another as in the case of a DT filled glass micro balloon. In an Eulerian calculation, the mesh remains fixed and the fluid flows through it so as time progresses, zones near the original DT-glass interface will contain both glass and DT. Very fine Eulerian zoning would be necessary near the interface to maintain spatial resolution and the average properties of the DT-glass mixture would be difficult to determine. There is no mixing in Lagrangian coordinates hence no averaging must be done. Since mesh points follow the fluid in a Lagrangian calculation, there tends to be more mesh points in steep density gradients and fewer points where the gradient is small just as there should be to maintain good resolution. These considerations most often outweigh the disadvantages of zone distortion.

The other independent variable is the time step, Δt, which has already been mentioned in the discussion of stability. Time steps must be computed by the hydrodynamics code because the characteristic time scale may vary

orders of magnitude throughout the course of a calculation. While the implosion process occurs in nanoseconds (10^{-9} sec), the thermonuclear burn phase is through in a few picoseconds (10^{-12} sec) after ignition.

III. Transport Equations

In addition to plasma hydrodynamics several transport processes should be considered when modelling laser fusion plasmas. These include radiative transfer, suprathermal electron transport, and charged particle fusion reaction product transport. Reaction neutron product transport might also be important for very high density pellets. Each of these particles possesses a mean-free-path that is considerably longer than the characteristic scale length of the hydrodynamic background plasma (at least in parts of the plasma). This behavior rules out the possibility of treating these species within the hydrodynamic framework. These particles are treated as separate species that interact with the plasma fluid through gain and loss terms in the temperature equations and through a momentum source term in the equation of motion. With many particles "created" and "destroyed" by thermonuclear reactions and heating of thermal electrons up into the suprathermal distribution, the continuity equation must also have a gain and loss term

$$\frac{\partial \rho}{\partial t} + \nabla \cdot \rho = G - L. \tag{11}$$

In practice, in Lagrangian coordinates, mass is automatically conserved by the zones so this gain and loss computation is really a matter of bookkeeping.

The transport of radiation will not be discussed in detail, except to point out some of the standard methods of solution. If the radiation mean-free-path is short enough the distribution function may be assumed

to be the local thermal Planckian distribution and the radiation can be characterized by its own temperature and temperature diffusion equation. This treatment is consistent with the hydrodynamic treatment of the plasma fluid. The transport equation itself can also be directly solved using S_N or Monte Carlo techniques. These can be very expensive to use in a time dependent problem and are used only in special cases. The transport equation can be expanded in angular moments to produce a diffusion equation or the P_N equations. The multi group diffusion equation must be flux limited to account for long mean-free-paths or the P_1 equations can be solved for the frequency dependent energy density and energy flux, the so called Variable Eddington method.[23]

More peculiar to laser fusion, however, are the transport of suprathermal electrons and charged particle reaction products. Suprathermal electrons play a significant role in the pellet implosion process for they are created by laser light absorption near the critical density in the underdense corona region of the plasma and stream inward carrying their energy into the dense plasma core. With energies in excess of 100 keV they may not be stopped until they stream through the ablation front into the cold adiabatically compressed plasma ahead of the front. This will heat up the cold plasma resulting in non-adiabaticity and a degradation of the implosion. To remedy this situation pellets are designed with high Z material surrounding the DT fuel that serves both as a tamper/pusher to enhance the implosion and as a shield against the suprathermal electrons and high frequency X-rays. Reaction product charged particles are principally ${}_1T^3$, ${}_2He^3$, ${}_1H^1$, and ${}_2He^4$ from the reactions

$$ {}_1D^2 + {}_1T^3 \rightarrow {}_2He^4\ (3.5\ \text{MeV}) + {}_0n^1\ (14.1\ \text{MeV}) \qquad (12) $$

and

$$ {}_1D^2 + {}_1D^2 \begin{cases} {}_2He^3\ (.82\ MeV) + {}_0n^1\ (2.45\ MeV) \\ {}_1T^3\ (1.01\ MeV) + {}_1H^1\ (3.02\ MeV) \end{cases} \qquad (13) $$

The temperature of the burning DT plasma is typically 4-100 keV so each of the reaction products is nonthermal.

The method that has received the greatest use to date for the transport of these nonthermal particles in a laser fusion hydrodynamics code is multi-group, flux-limited diffusion theory. This method is used in LASNEX, a two dimensional Lagrangian hydrodynamics code written at Lawrence Livermore Laboratory.[24] Flux limited diffusion uses a diffusion equation to model transport with a flux corrected diffusion coefficient to account for long mean-free-path situations. The slowing down is done in a multi group structure so the equations look like[25]

$$ \frac{\partial N_g}{\partial t} - \nabla \cdot D_g \nabla N_g + L_g N_g = S_g \qquad g = 1, \ldots, G \qquad (14) $$

where $N_g(\underline{r},t)$ is the density of particles with energies between E_g and E_{g-1} in d^3r at time t, and L_g is some slowing down operator that removes and adds particles from energy group g. Several questions concerning the applicability of these equations to charged particle transport must be answered.

(1) How should the transport cross section in the diffusion coefficient be defined?

(2) How should the slowing down operator be defined?

(3) How good is the diffusion approximation and how does flux limiting help?

(4) How good is the multigroup structure for this type of slowing down problem?

The answers to the first two questions come from the Fokker-Planck equation. This equation describes the evolution of the charged particle distribution function, $f_\alpha(\underline{r},\underline{v},t)$, where α denotes the particular species of particle being transported. The equation takes the form

$$\frac{\partial f_\alpha}{\partial t} + \underline{v} \cdot \frac{\partial f_\alpha}{\partial \underline{r}} + \frac{\underline{F}_\alpha}{m_\alpha} \cdot \frac{\partial f_\alpha}{\partial \underline{v}} = \left(\frac{\delta f_\alpha}{\delta t}\right)_c \tag{15}$$

where $\underline{F}_\alpha = q_\alpha\ (\underline{E} + \underline{v} \times \underline{B})$ and

$$\left(\frac{\delta f_\alpha}{\delta t}\right)_c = \frac{\partial}{\partial \underline{v}} \cdot \left(\underline{\underline{K}} \cdot \frac{\partial f_\alpha}{\partial \underline{v}} - \underline{L}\ f_\alpha\right) \tag{16}$$

where $\underline{\underline{K}}$ and $\underline{L}$ are the velocity space diffusion and drag terms. Due to the long range of the Coulomb potential charged particles slow down through many small angle scattering events. The right hand side of this equation models this process and is significantly different than the corresponding term in neutron transport. Solution of the Fokker-Planck equation in an infinite medium will yield several characteristic transport times (or lengths) of interest. The first is the time (or length) that a fast particle takes to deflect through an angle of 90°, which we call τ_D. For ions streaming through a thermal plasma this is

$$\tau_D = \frac{\sqrt{m/2}\ E^{3/2}}{2\pi\ Z^2\ e^4\ \ln\Lambda_I \sum_i Z_i^2\ n_i} \tag{17}$$

where m, E, and Z are the mass, energy, and charge of the fast particle and Z_i and n_i are the charge and density of the i^{th} ionic species. Using this time, a macroscopic transport cross section can be defined as

$$\Sigma_{tr} = \frac{1}{v\tau_D} \tag{18}$$

and the multigroup diffusion coefficient is given as

$$D_g = \frac{v_g}{3\Sigma_{tr_g}} = \frac{v_g}{3/v_g\ \tau_{Dg}} \quad . \tag{19}$$

The time τ_D is obtained from the Fokker-Planck equation by considering the $\underline{\underline{K}}$ term in the collision model. This term changes the distribution function by relaxing it toward isotropy.

The slowing down of particles will depend on both the $\underline{\underline{K}}$ and $\underline{L}$ terms in the Fokker-Planck equation. For fast ion transport at high energy the $\underline{L}$ term will dominate and will be due to interactions with electrons but as the fast ion slows down the $\underline{\underline{K}}$ term will dominate and slowing will be due to larger angle collisions with the thermal ions. In Fig. 7 dv/ds is plotted for the thermal electron and ion contributions as a function of fast particle velocity. The domination of the electrons at high energy and ions at low energy is clearly seen.

If we let

$$\frac{dv}{dt} = V \frac{dv}{ds} \tag{20}$$

and define

$$\tau_g = v_g/(dv_g/dt) \tag{21}$$

then the slowing down operator can be expressed as

$$L_g = N_g/\tau_g - N_{g-1}/\tau_{g-1} \tag{22}$$

and the multigroup diffusion equations are written as

$$\frac{\partial N_g}{\partial t} - \nabla \cdot D_g \nabla N_g + N_g/\tau_g - N_{g-1}/\tau_{g-1} = S_g,\ g = 1, \ldots, G \tag{23}$$

where we assume particles can only scatter into group g from the next higher energy group, and when particles reach thermal energies they are added back into the hydrodynamic thermal plasma.

The answer to the third question is, of course, that diffusion theory is not a very good transport approximation, however, it is partially corrected

by flux limiting. Recall that the diffusion equation is obtained from the particle continuity equation

$$\frac{\partial N}{\partial t} + \nabla \cdot \underline{Q} + L\ N = S \tag{24}$$

by using the transport law

$$\underline{Q} \simeq - D\nabla N. \tag{25}$$

In the free streaming limit

$$\underline{Q} = \underline{v}N \tag{26}$$

and this is the maximum flux that could arise.

In the situation where

$$N/(\nabla N) < \lambda_{mfp}, \tag{27}$$

that is in the transport regime

$$|\underline{Q}| = D\nabla N > \underline{v}N. \tag{28}$$

This unphysical problem can be avoided by redefining the transport law as

$$\underline{Q} = \frac{- D\ \nabla N}{1 + \left|\frac{\tilde{D}\nabla N}{Q_{max}}\right|} = - \tilde{D}\nabla N \tag{29}$$

where Q_{max} is chosen in some appropriate way to correspond to the flux in the free streaming limit. This ad-hoc diffusion coefficient will insure physically plausible transport of the particles, for when diffusion theory holds

$$\frac{\tilde{D}\nabla N}{Q_{max}} << 1 \tag{30}$$

so

$$\underline{Q} = - D\nabla N \tag{31}$$

and when mean-free-paths are very long

$$\frac{\tilde{D\nabla N}}{Q_{max}} >> 1 \tag{32}$$

and

$$\underline{Q} = Q_{max} \left(\frac{-D\nabla N}{|\tilde{D\nabla N}|}\right) \tag{33}$$

where the quantity in brackets is a unit vector.

The accurate slowing down of charged particles by multigroup methods can be a problem. This is a continuous slowing down process with a strong coupling between the energy, space and time variables. This can result in a great deal of numerical diffusion in energy space, with as many as 100 groups required to give reasonable accuracy.

The multigroup equations are also only first order accurate in the energy variable and are usually only first order accurate in time as well, because a fully implicit differencing scheme must be used to allow the hydrodynamic time step to be used:

$$\frac{N_g^{n+1} - N_g^n}{\nabla t^{n+1/2}} = \nabla \cdot D_g \nabla N_g^{n+1} - N_g^{n+1}/\tau_g + N_{g-1}^{n+1}/\tau_{g-1} + S_g^{n+1/2} \quad . \tag{34}$$

This, of course, is a general scheme that can be used to model almost any kind of particle transport. It produces reasonably good results for non-diffusive problems and is very straightforward to implement numerically, even in two dimensions. It embodies the essentials of most transport problems and should give reasonable answers for integrated quantities, such as total reaction rates. But even in 1977 there still is no such thing as a free lunch so care should be taken when interpreting detailed results of the flux limited diffusion treatment of transport dominated problems. Over less than a mean-free-path, as will be seen next, flux limited diffusion can miss details entirely for certain types of problems.

An alternative approach to charged particle transport is to use techniques that are specifically adapted to the behavior of the particular charged particles. In Fig. 8, borrowed from the paper by N. Winsor, we see that the ion beam streaming through a background plasma has less dispersion in velocity space than the electron beam. The electron beam becomes much more isotropic as it slows down due to large angle scattering; however, the ion beam simply slows down without much scattering out of the beam trajectory, $v_{//}$. The electron behavior tends to reinforce the applicability of flux limited diffusion theory as a description of the electron transport for that treatment demands that the distribution function be nearly isotropic. In the case of thermonuclear reaction products, however, the ion beam results indicate that isotropy is not reached until near the end of the particles' path to thermalization. This behavior can be used to great advantage in modelling the reaction product transport for it says that a simple straight line trajectory will be a good approximation. This is the basic assumption used in the time dependent particle tracking algorithm.

In a one-dimensional Lagrangian hydrodynamic treatment, the spherical plasma is divided into concentric shells or "zones" and the plasma behavior is represented by the finite difference solution to the equations for density, fluid velocity, and electron and ion temperature as discussed in part II. To model the charged particle fusion reaction products ($_1T^3$, $_2He^3$, $_1H^1$, $_2He^4$), it is assumed that those created in each zone stream along a finite number of rays that originate in the center of the zone, Fig. 9. As the stream they

experience the Coulomb drag force represented by the $\underline{L}$ terms in the Fokker-Planck equation, Eqn. 15 , and a range-energy relation can be expressed in the following form[26]

$$\frac{-dv}{ds} = A + B/v^3 = K(v) \tag{35}$$

$$A = A_o\ (Z^2/m)\ \ell n\ \Lambda_e\ n_e/T_e^{3/2}$$

$$B = B_o\ (Z^2/m)\ \ell n\ \Lambda_i\ \sum_i Z_i^2\ n_i/\rho$$

where the A term is due to scattering on the thermal electrons and the B term is for the thermal ions. This is the expression plotted in Fig. 7. The straight line trajectory will be valid during most of the slowing down process; however, near the end, the fast particle loses its energy in large angle collisions with thermal ions. This inaccuracy is mitigated, however, by recognizing the purpose of the transport problem. In the transport of fusion reaction products, it is the energy redeposition back into the thermal electrons and ions that is of greatest importance and near the end of a reaction product's trajectory it has very little energy remaining; hence, the error in redeposition is small. Eqn. 35 is solved along a ray as it passes from one zone boundary to the next by integrating it along its exact path length[26]

$$\Delta s = \int_{v_o-\Delta v}^{v_o} g(v)\ dv \tag{36}$$

where Δs is the distance across the zone along the particle trajectory, v_o is the particle velocity on entering the zone, Δv is the velocity loss in crossing the zone, and

$$g(v) = [K(v)]^{-1} \quad . \tag{37}$$

The A and B terms are evaluated using the temperature and density of the zone. Eqn. 36 is an integral equation for Δv and can be solved using a Taylor expansion

$$g(v) \simeq g(v_o) + (v-v_o)\, g'(v_o) \tag{38}$$

$$= g_o + (v-v_o)\, g_o' \quad .$$

Substitution into Eqn. 36 yields

$$\Delta s \simeq g_o \Delta v - 1/2\, g_o' \, (\Delta v)^2 \quad . \tag{39}$$

This expression can be inverted and solved to second order for Δv as

$$\Delta v = \Delta s/[g_o(1 - 1/2\, g_o'/g_o^2\, \Delta s)] \tag{40}$$

or equivalently

$$\Delta v = K(v_o)\, \Delta s/[1 + 1/2\, K'(v_o)\, \Delta s] \quad . \tag{41}$$

This procedure is accurate for $\Delta v/v_o << 1$; however, should $\Delta v/v_o \geq 1$, then the particles have thermalized within the zone so again the error to energy redeposition will not be serious. Only the partition of energy

to the electrons and ions will be important. The total energy lost in a zone is simply

$$\Delta E = 1/2\ m\ [v_o^2 - (v_o - \Delta v)^2]\ N \tag{42}$$

where N is the number of ions streaming along a given ray. The fraction of this energy going to the electrons is

$$\Delta E^{(e)} = A\ (\Delta s/\Delta v)\ \Delta E\ . \tag{43}$$

Should the particles slow to thermal energy in the zone ($\Delta v/v_o \sim 1$), then the fraction of energy going to electrons can be obtained from the results of an infinite medium calculation, tabulated as a function of electron temperature. Then the loss to ions in either case is

$$\Delta E^{(i)} = \Delta E - \Delta E^{(e)}\ . \tag{44}$$

In addition to energy redeposition, the nonthermal ions also impart momentum to the zone

$$m\ \Delta v\ N\ \cos\alpha = M\ \Delta u \tag{45}$$

where M is the zone mass, m is the nonthermal particle mass, and α is the angle between the trajectory of the ions and the outward radial direction. The algorithm to compute the energy redeposition from the reaction product ions would then simply be

```
FOR EACH REACTION PRODUCT                                    (46)
   FOR EACH ZONE
      FOR EACH RAY
                                  TRACK ION TRAJECTORIES FROM
                                  CREATION TO THERMALIZATION OR
                                  ESCAPE AND TALLY THE AMOUNT OF
                                  ENERGY AND MOMENTUM DEPOSITED
                                  IN EACH ZONE ALONG THEIR PATH
      END
   END
END
```

To advance the solution to the hydrodynamics equations by one time step, the reaction rate equations must be solved for each zone and the particles produced on this time step divided among the different rays. Then the three nested loops must be executed to determine the amount of energy and momentum deposited in each zone. This information can then be used as a source term in the hydrodynamic equations. This algorithm is very simple and is straightforward to implement in a hydrodynamics computer code. It does not use any finite difference methods and suffers from no numerical instabilities.

The particle tracking algorithm discussed thus far has assumed an "adiabatic" approximation to the time dependence of the slowing down.[26] Specifically, a slowing down calculation is done for each time step in the

hydrodynamics calculation. The fast ions are "forced" to thermalize or escape the plasma during the time step on which they are created. This is, of course, an assumption which must be tested for its validity. A 3.5 MeV alpha particle has an initial velocity of 13 μm/psec. If this particle was born near the hot center of an otherwise cold pellet core, it may need to travel 15 μm before it is slowed appreciably by the surrounding cold plasma. Assuming no energy loss in the hot central "microcore," this particle will require 1.15 psec to reach the cold plasma, a time that is easily greater than typical time steps in a thermonuclear burn-hydrodynamics computation. In such calculations, time steps often are as short as 0.01 psec so we see that the "adiabatic" approximation is not necessarily a good one; however, the only real proof is to compare it to a fully time dependent calculation. The particle tracking method can be made time dependent at the sacrifice of its delightful simplicity. To do this we note that a "bunch" of particles (say alphas) created at position $r_{j-1/2}$ at time $t^{n+1/2}$ and traveling along a ray in direction μ_m can be totally characterized by four numbers: the number of particles in the "bunch," N; the position of this bunch of particles, R; the direction of these particles with respect to the radius vector to position R, μ; and the velocity of the particles, V. These are displayed in Fig. 9. Particles can now be "tracked" from their origin or birth place to the position that they reach after a time Δt, the hydrodynamic time step. At this time their new position, direction, velocity, and number of them can be "remembered" until the next time step. Such an algorithm requires that the energy-time relationship be integrated along the rays also.

$$-\frac{dv}{dt} = \frac{-vdv}{ds} = Av + B/v^2 = J(v) \ . \tag{47}$$

In exact analog to the solution of Eqn. 36, Eqn. 47 can be integrated to give

$$\Delta v = J_0 \Delta t / [1 + 1/2 \ J_0' \ \Delta t] \ . \tag{48}$$

In addition to these relations, we must also know the distance travelled in a time Δt and the time taken to move a distance Δs. These are given by

$$\Delta t_{\Delta s} = (\Delta v/J_0) + 1/2 \ J_0' \ (\Delta v/J_0)^2 \tag{49}$$

$$\Delta s_{\Delta t} = (\Delta v/K_0) + 1/2 \ K_0' \ (\Delta v/K_0)^2 \ . \tag{50}$$

The algorithm to compute the time dependent transport is considerably more complicated than in the time independent case and is shown in Fig.10.

```
FOR EACH REACTION PRODUCT
   FOR EACH ZONE
      FOR EACH RAY
         FOR EACH PAST TIME LEVEL                    (51)
            (SEE FIG. 10)
         END
      END
   END
END
```

This algorithm involves remembering the positions, directions, and velocities of particles created on previous time steps that are still streaming. To save all of this information will require N_s words of computer memory, where

$$N_s = N_Z \times (N_A^+ N_T^+ + N_A^- N_T^-) \times N_p \times 4$$

and

N_Z = number of zones

N_A^+ = number of directions with $\mu > 0$

N_A^- = number of directions with $\mu \leq 0$

N_T^+ = number of time steps to remember particles starting in a $\mu > 0$ direction

N_T^- = number of time steps to remember particles starting in a $\mu \leq 0$ direction

N_p = number of different kinds of particles to be tracked.

The number of time steps necessary to follow particles starting in an outward direction will be less than the number required for inward directed particles so provision is made to optimize the amount of necessary storage by utilizing this fact. Also, with such a scheme, there is always the possibility that a group of particles that have been remembered for $N_T^{\pm}$ future time steps will

neither have thermalized or escaped the plasma. In such a case, these particles are forced to thermalize or escape by using the adiabatic approach discussed previously. In practice, enough storage can usually be provided to minimize the effects of this problem. The advantage of this time dependent particle tracking algorithm is the good treatment of the slowing down process and energy redeposition at a very reasonable cost. The disadvantage is the rather complex logic required to execute the algorithm necessitating very careful programming.

The first test of the TDPT algorithm is really a test of the accuracy of the slowing down treatment. In this test the energy redeposition to electrons and ions as a function of position from a point source of 3.5 MeV alphas is computed using TDPT, Monte Carlo, and flux limited, 100 group diffusion theory. The results shown in Fig. 11 indicate that the TDPT algorithm reproduces the most accurate Monte Carlo results much better than flux limited diffusion theory. Since the behavior displayed in Fig. 11 occurs in a distance less than one collision mean-free-path with an electron, we would expect that a transport theory treatment is necessary to describe it and this is in fact the case. Flux limited diffusion theory, even with 100 groups, is unable to even qualitatively reproduce the ion redeposition results. Time dependent particle tracking reproduces the Monte Carlo results remarkably well considering that the electron temperature in this example was chosen to be 50 keV. At such electron temperatures the straight line approximation to the fast ion trajectory is not necessarily good; however, the "Bragg peak" in the redeposition to the thermal ions is predicted by the TDPT method with

nearly the correct amplitude and position from the origin. The straight line approximation forces the peak to be a little further from the origin and also narrower than the Monte Carlo result because no back-scatter is allowed.

The second test of the TDPT method involves the sensitivity of integrated burn results to changes in important parameters in the TDPT model. The results to be studied are total number of 14 MeV neutrons produced and total number of alpha particles escaping from a 3 g/cm^2 pellet core. These are computed using simulations with varying values of initial directions, number of remembered time steps and minimum allowable time step. The results shown in Fig. 12 indicate that the total number of neutrons produced from DT reactions is insensitive to the variation of these parameters. The worst deviation is when only one time level is remembered, which is equivalent to the adiabatic approximation. Even here the deviation is not great. The number of escaping alpha particles is rather insensitive to these parameters also, except for the case of the adiabatic approximation. Here the number of escaping particles is grossly overestimated; however, as noted earlier, the yield is about the same as the other more exact time dependent problems. These calculations are for a 1 mg,3 g/cm^2 pellet core so the conclusion is that the ultimate yield of a nonmarginal pellet core is not sensitively dependent on the parameters used in the TDPT transport method; however, the number of escaping particles can be affected so care must be taken if escaping charged particle spectra are computed.

The final result is a comparison with a full thermonuclear burn-hydrodynamics calculation. In this case the PHD-II result is within about 15% of

the final yield of the comparison calculation, Fig. 13. This indicates that the TDPT method coupled to a hydrodynamics code, PHD-II, gives results comparable to discrete ordinates transport of the charged particles.

The discussion in this section has centered on two different transport methods. One presumes diffusion and corrects for streaming and the other presumes streaming and must correct for large angle scattering. From Fokker-Planck studies of the detailed behavior of charged particles, it would seem that flux limited diffusion is most applicable to the suprathermal electron transport while the time dependent particle tracking does very well for nonthermal ion transport.

IV. Summary

Laser fusion hydrodynamics and transport is a relatively new field that has room for much more development. This is apparent from the very few laser fusion codes that exist today. The most notable and complete code is LASNEX with two-dimensional Lagrangian hydrodynamics and flux limited diffusive transport. Another 2-D code with a sophisticated treatment of magnetic fields and radiative processes is LASMAP, an Eulerian code written at NRL. Each of the principle laboratories involved with laser fusion research also have their own one-dimensional code.

As more experiments are being undertaken, it becomes increasingly apparent that so-called anomalous effects are not just a first order correction to the classical hydrodynamics problem but are in fact dominating the results. To model these processes will require the treatment of particle distribution functions that may be far from equilibrium. Flux limited multi-group diffusion is a first attempt to include these effects in a hydrodynamics code; however, the necessity of "knob-turning" in the codes in order to obtain good agreement with experiment and the sensitivity of results to numerical parameters such as zoning, time steps and differencing techniques makes one pause and wonder whether these simple models can afford good insight into laser plasma dynamics. The detailed treatment of particle distribution functions and numerical schemes designed for accuracy rather than expediency imply a great increase in computer time for codes that already use large amounts of it. One solution must be to implement these codes

with numerical algorithms that are optional on the new generation of vector processing machines (TI-ASC, CDC-STAR, CRAY-I, etc.). Another partial solution may be to develop more codes or large modular codes that accurately treat very specific problems. This may seem inefficient; however, a code that is designed with enough generality to solve any kind of problem is probably going to give away too much to expediency to do the best job on any specific problem, and these nonlinear equations are very unforgiving to inaccuracies in physics or numerics. The present codes are very valuable, though, and must continue to be used to point out sensitive and insensitive processes as a guideline for further development.

REFERENCES

1. J. Nuckolls, L. Wood, A. Thiessen and G. Zimmerman, Nature 239, 139 (1972).

2. J. Clarke, H. Fisher and R. Mason, Phys. Rev. Lett. 30, 89 (1973).

3. K. Brueckner and S. Jorna, Rev. Mod. Phys. 46, 325 (1974).

4. G. Fraley, E. Linnebur, R. Mason and R. Morse, Phys. Fl. 17, 474 (1974).

5. J. Friedberg, R. Mitchell, R. Morse and L. Rudsinski, Phys. Rev. Lett. 28, 795 (1972).

6. J. Howard, UWFDM-188, (1976). (Submitted to Nuclear Fusion).

7. R. Morse and C. Nielson, Phys. Fl. 16, 909 (1973).

8. T. Tan, G. McCall, A. Williams, D. Giovanielli and R. Godwin, Bull. Am. Phys. Soc. 21, 1047 (1976).

9. J. Lindl, Nucl. Fus. 14, 511 (1974).

10. R. Malone, R. McCrory and R. Morse, Phys. Rev. Lett 34, 721 (1975).

11. J. Stamper and J. Dawson, Phys. Rev. Lett. 26, 1012 (1971).

12. S. Braginskii, Review of Plasma Physics, Vol. I, 205 (Consultants Bureau, 1965).

13. J. Shiou, E. Goldman and C. Weng, Phys. Rev. Lett, 32, 352 (1974).

14. D. Henderson and R. Morse, Phys. Rev. Lett., 32, 355 (1974).

15. D. Henderson, R. McCrory and R. Morse, Phys. Rev. Lett. 33, 205 (1974).

16. J. Lindl and W. Mead, Phys. Rev. Lett., 34, 1273 (1975).

17. K. Brueckner, Nuc. Fus. 16, 387 (1976)
M. Stroscio, LA-6465-MS (1976).

18. B. Yaakobi, Bull. Am. Phys. Soc. 21, 1189 (1976).

19. L. Spitzer, Physics of Fully Ionized Gases (Wiley, 1962), 2nd Edition.

20. R. Richtmyer and K. Morton, Difference Methods for Initial Value Problems (Interscience, 1967), 2nd Edition.

21. J. Von Neumann and R. Richtmyer, J. Appl. Phys. 21, 232 (1950).

22. Y. Zeldovich and Y. Raizer, Physics of Shock Waves and High Temperature Hydrodynamic Phenomena, Vol. II, (Academic Press, 1966) p. 660.

23. P. Campbell, Int. J. Heat Mass Transfer 12, 497 (1969).

24. G. Zimmerman, Comments on Plasma Physics 2, 51 (1975).

25. E. Corman, W. Loewe, G. Cooper and A. Winslow, Nucl. Fus. 15, 377 (1975).

26. H. Brysk, KMSF Report U275 (1975).

FIGURE CAPTIONS

FIG. 1 - LASER FUSION PELLET SCENARIO

FIG. 2 - BURN WAVE PROPAGATION

FIG. 3 - LIGHT REFRACTION AT OBLIQUE INCIDENCE

FIG. 4 - COMPRESSION SENSITIVITY TO THERMAL CONDUCTION

FIG. 5 - TWO DIMENSIONAL LAGRANGIAN ZONE DISTORTION

FIG. 6 - TWO DIMENSIONAL LAGRANGIAN MESH

FIG. 7 - FAST ION RANGE-ENERGY RELATION

FIG. 8 - FOKKER-PLANCK CALCULATION

FIG. 9 - PARTICLE TRACKING ALONG RAYS

FIG. 10 - TIME DEPENDENT PARTICLE TRACKING ALGORITHM

FIG. 11 - COMPARISON OF TDPT, MONTE CARLO AND FLUX LIMITED DIFFUSION

FIG. 12 - SENSITIVITY OF TDPT TO NUMERICAL PARAMETERS

FIG. 13 - COMPARISON OF BURN CALCULATIONS USING TDPT AND S_N TRANSPORT

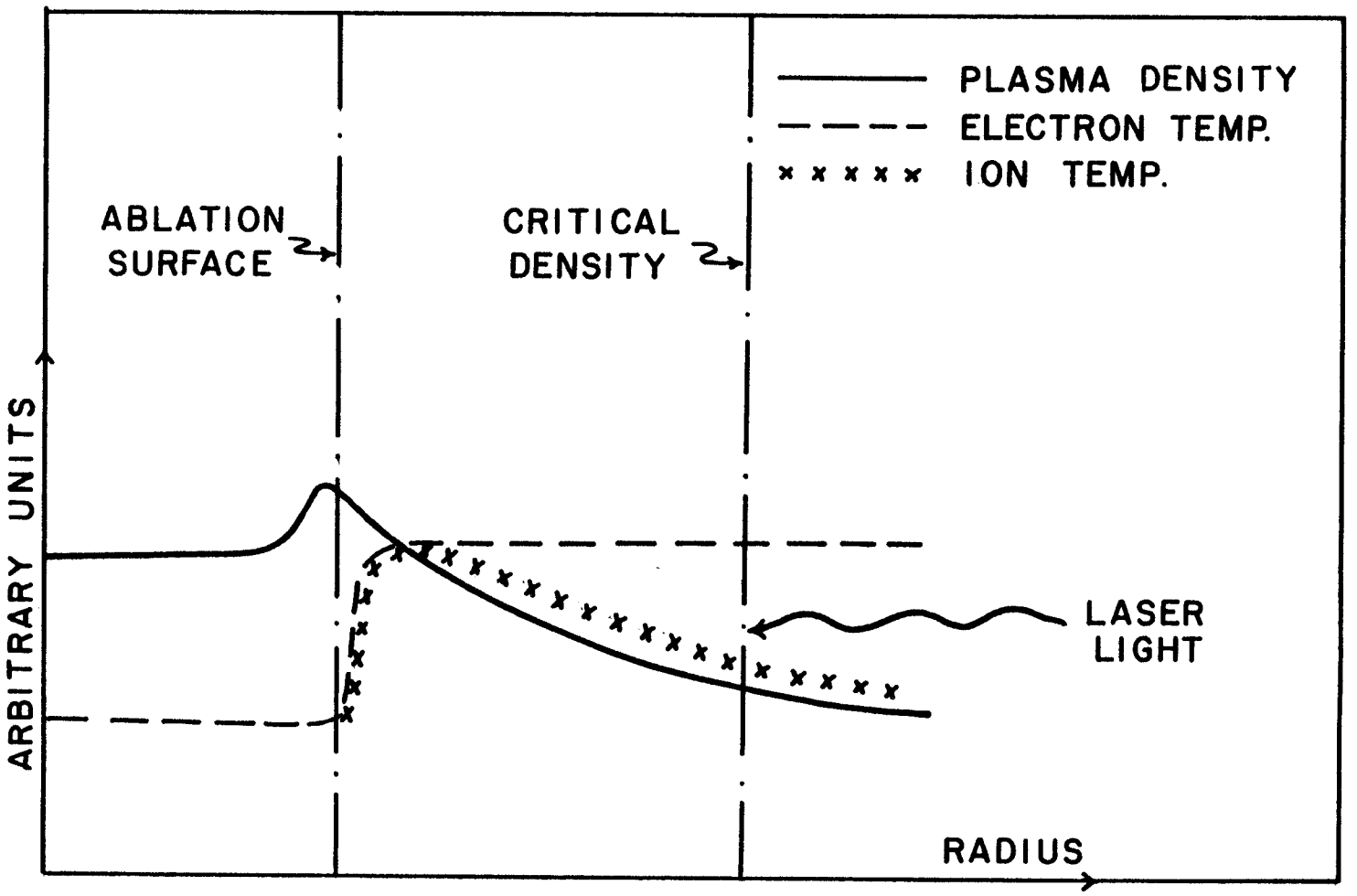

FIGURE 1 LASER-PELLET INTERACTION SCENARIO

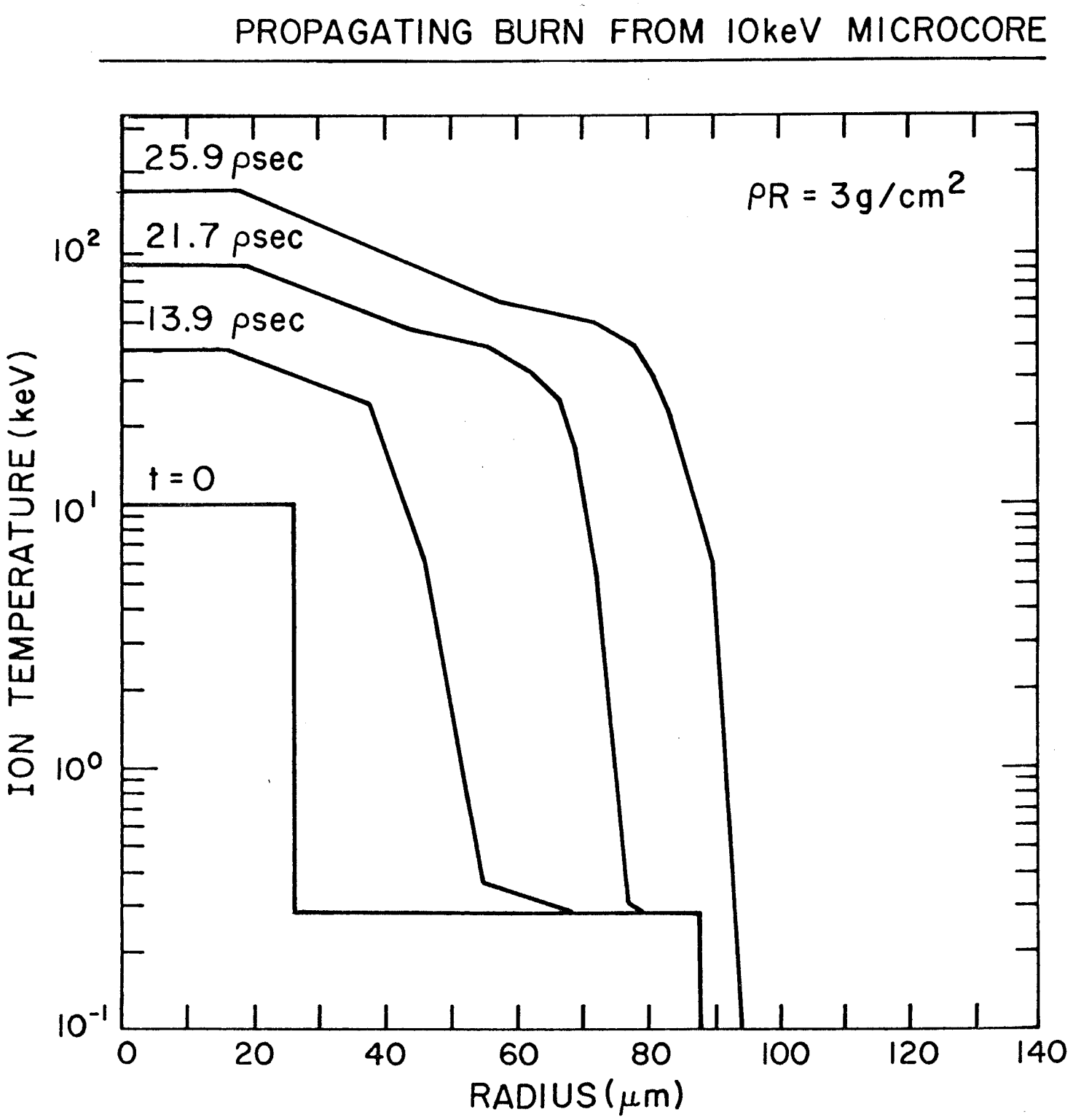
PROPAGATING BURN FROM 10keV MICROCORE
25.9 ρsec
21.7 ρsec
13.9 ρsec
t = 0
ρR = 3g/cm²
ION TEMPERATURE (keV)
10²
10¹
10⁰
10⁻¹
0
20
40
60
80
100
120
140
RADIUS (μm)

FIGURE 2

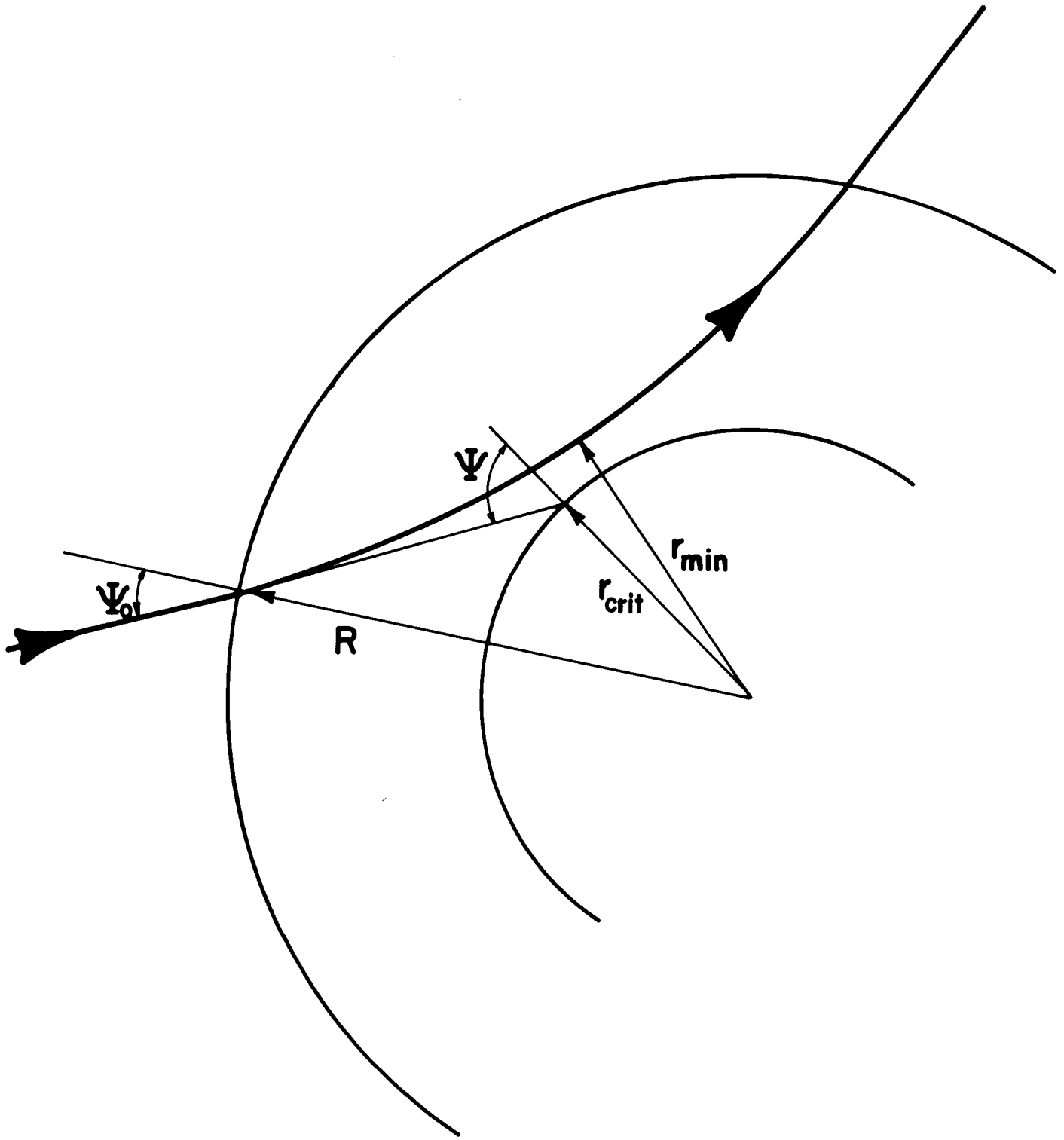

FIGURE 3

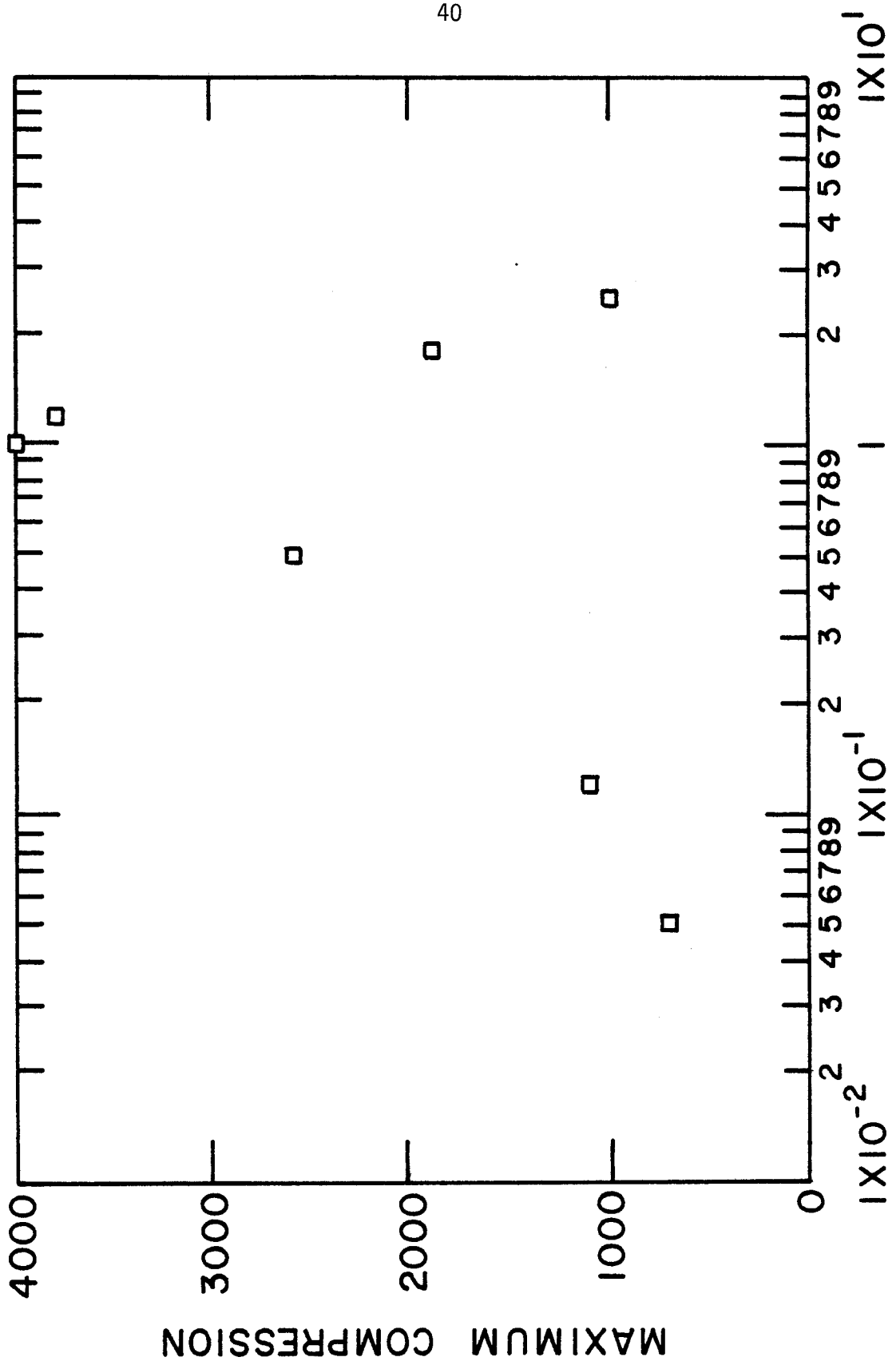
MAXIMUM COMPRESSION
4000
3000
2000
1000
0
1X10-2
2
3
4
5
6
7
8
9
1X10-1
2
3
4
5
6
7
8
9
1
2
3
4
5
6
7
8
9
1X10+1
K/<K>

FIGURE 4

LAGRANGIAN COORDINATES

- MESH IS IMBEDDED IN FLUID

CLASSIC PROBLEM

- ZONE DISTORTION

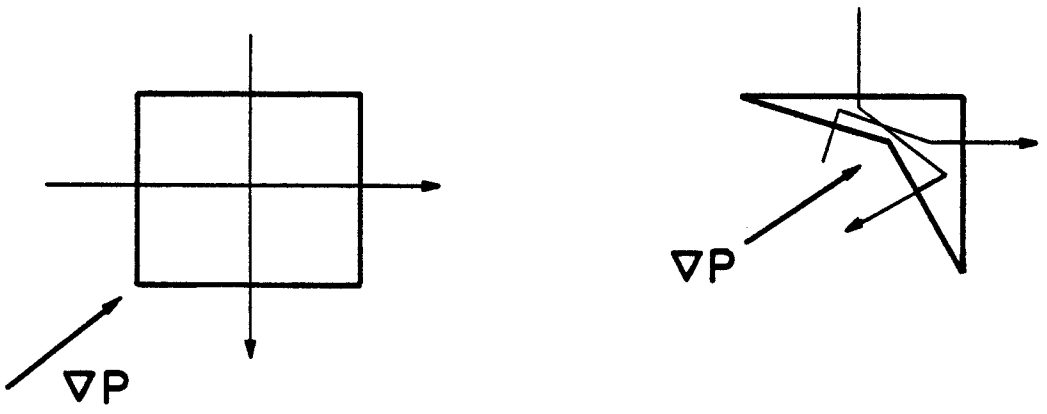

SOLUTION

- REZONING
- MIXED EULERIAN - LAGRANGIAN

ADVANTAGES

- BETTER RESOLUTION

FIGURE 5

TWO DIMENSIONAL ZONING

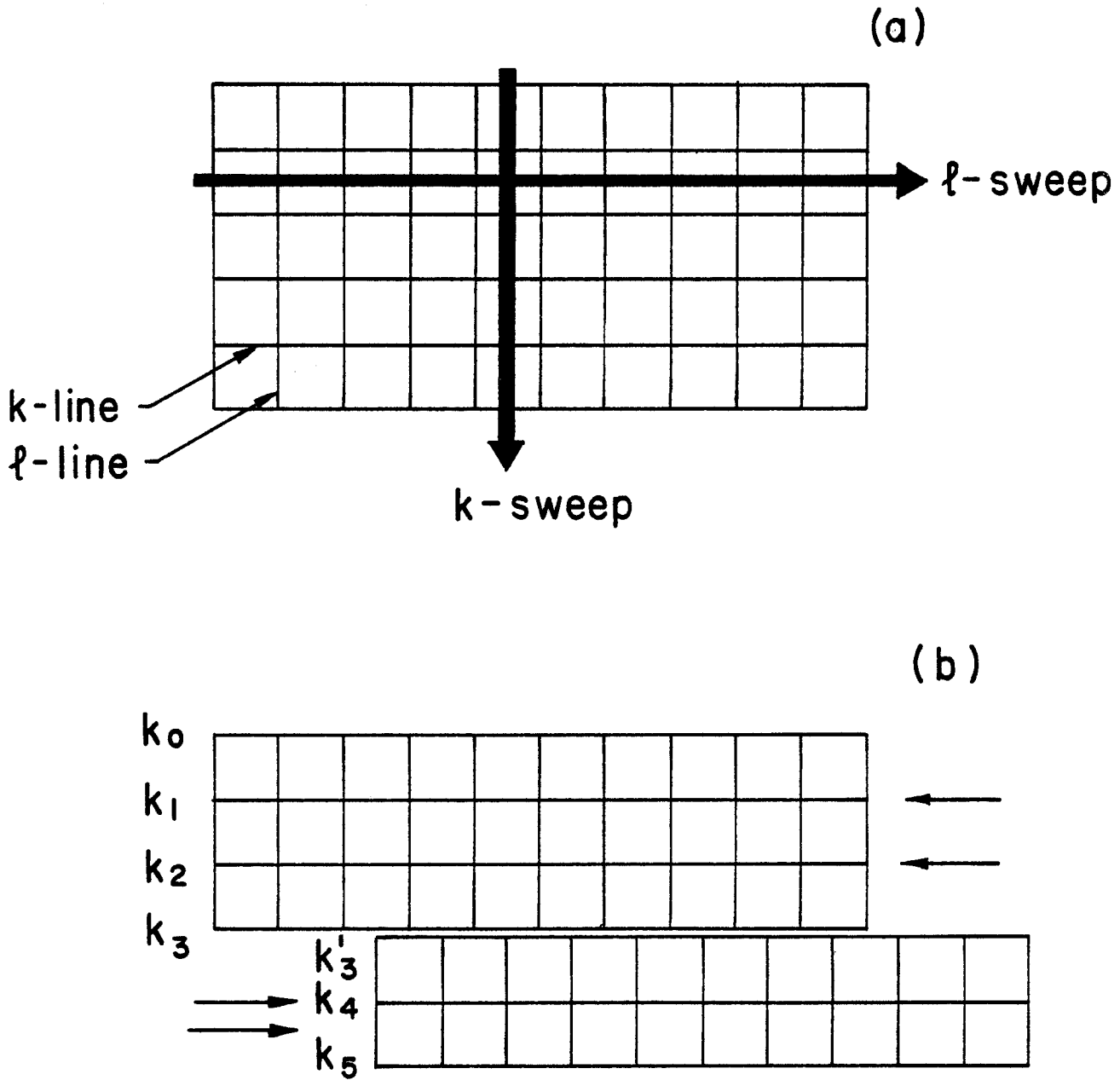

FIGURE 6

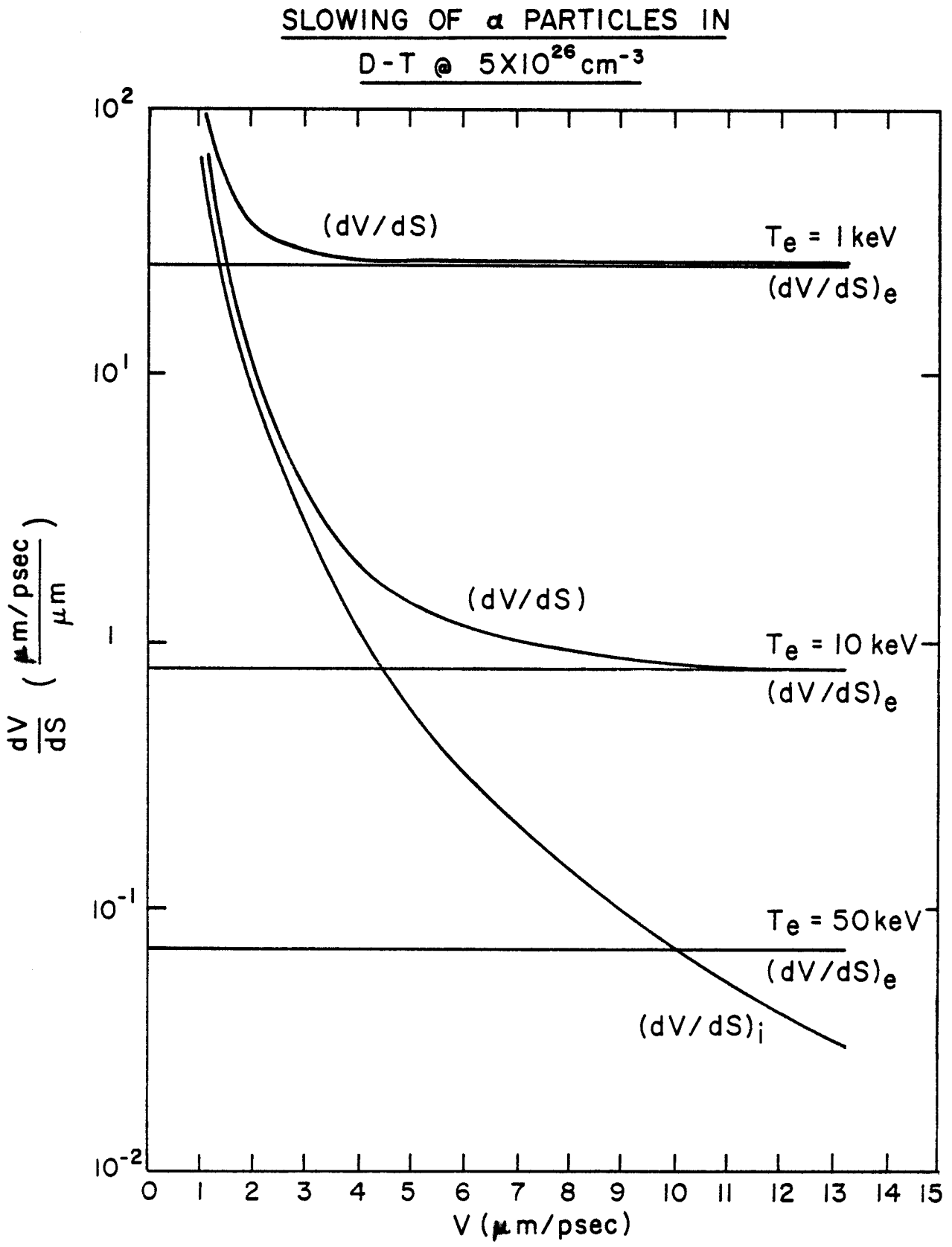
SLOWING OF α PARTICLES IN
D-T @ 5X10^26 cm^-3
10^2
10^1
1
10^-1
10^-2
dV/dS (μm/psec / μm)
(dV/dS)
Te = 1 keV
(dV/dS)e
(dV/dS)
Te = 10 keV
(dV/dS)e
Te = 50 keV
(dV/dS)e
(dV/dS)i
0 1 2 3 4 5 6 7 8 9 10 11 12 13 14 15
V (μm/psec)

FIGURE 7

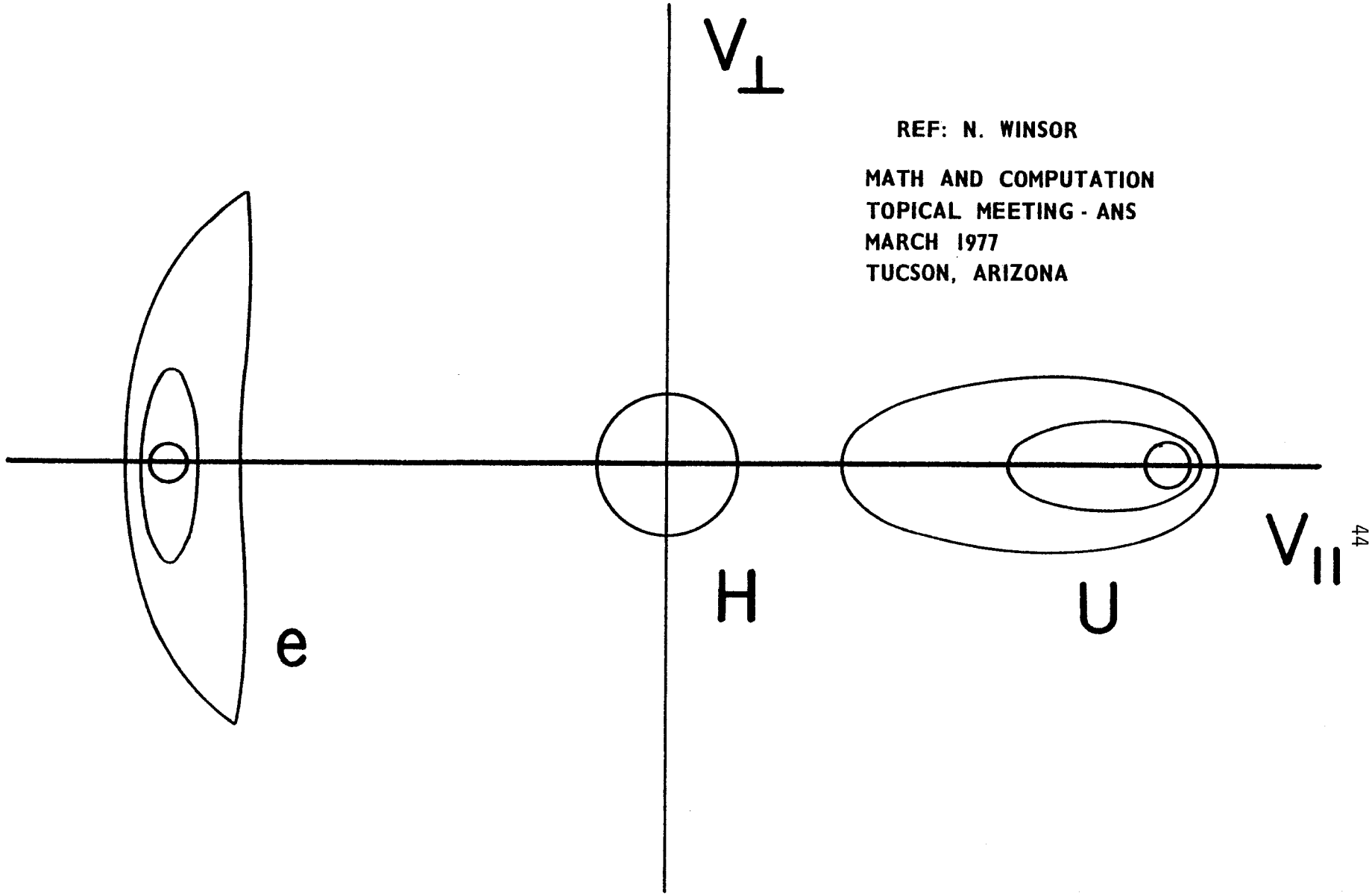

FOKKER-PLANCK CALCULATION

FIGURE 8

TIME DEPENDENT PARTICLE TRACKING

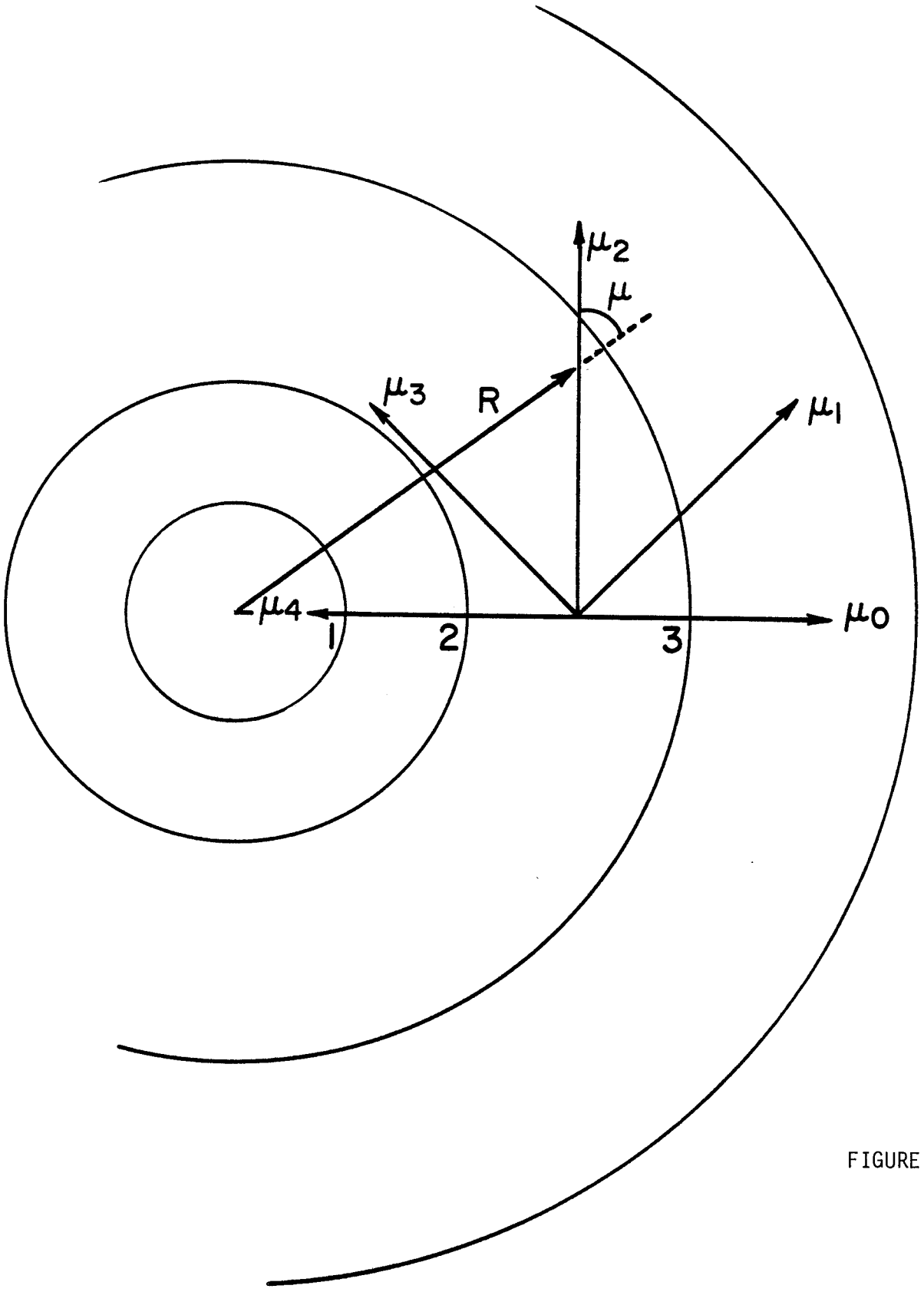

FIGURE 9

TIME DEPENDENT PARTICLE TRACKING ALGORITHM

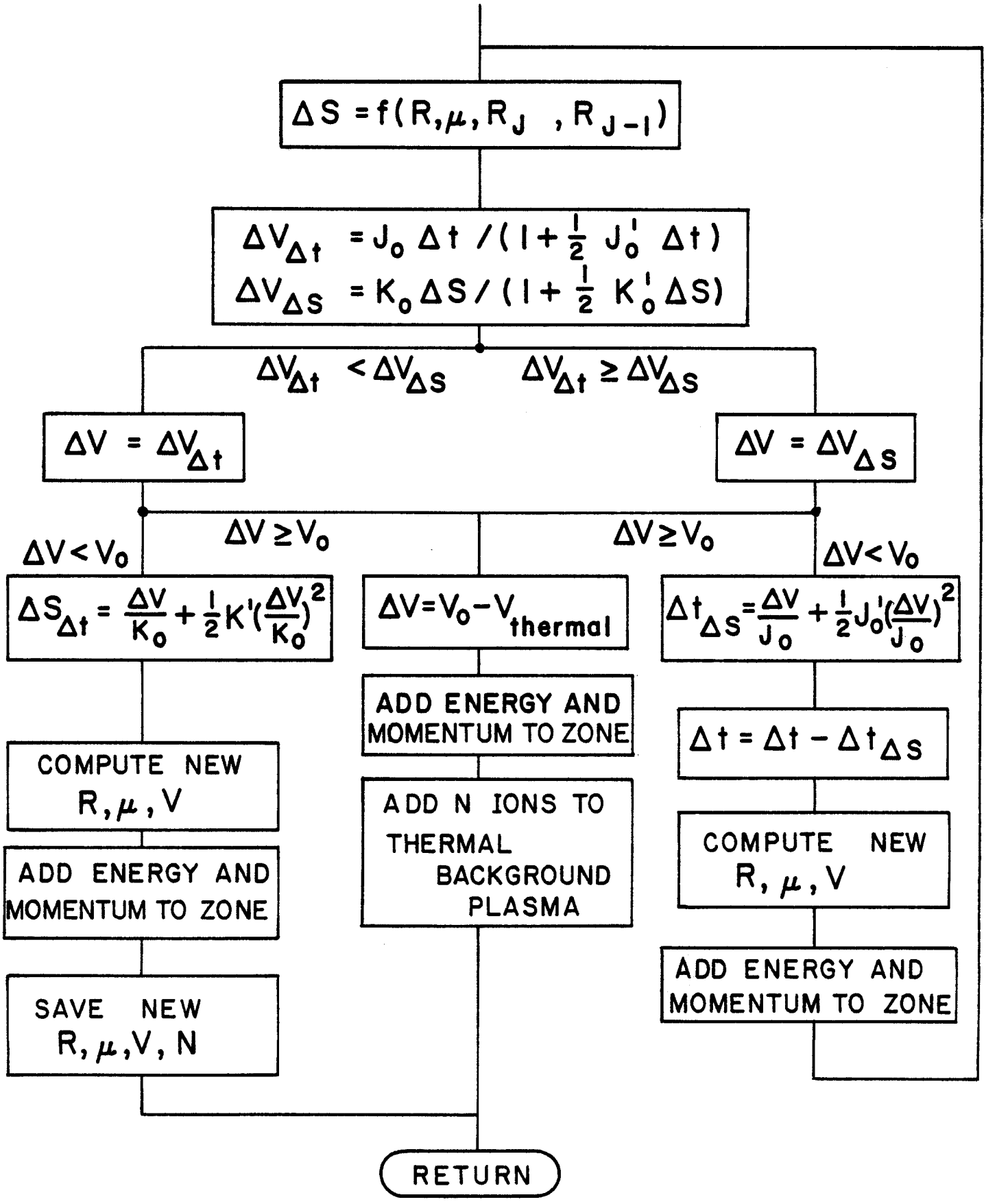

FIGURE 10

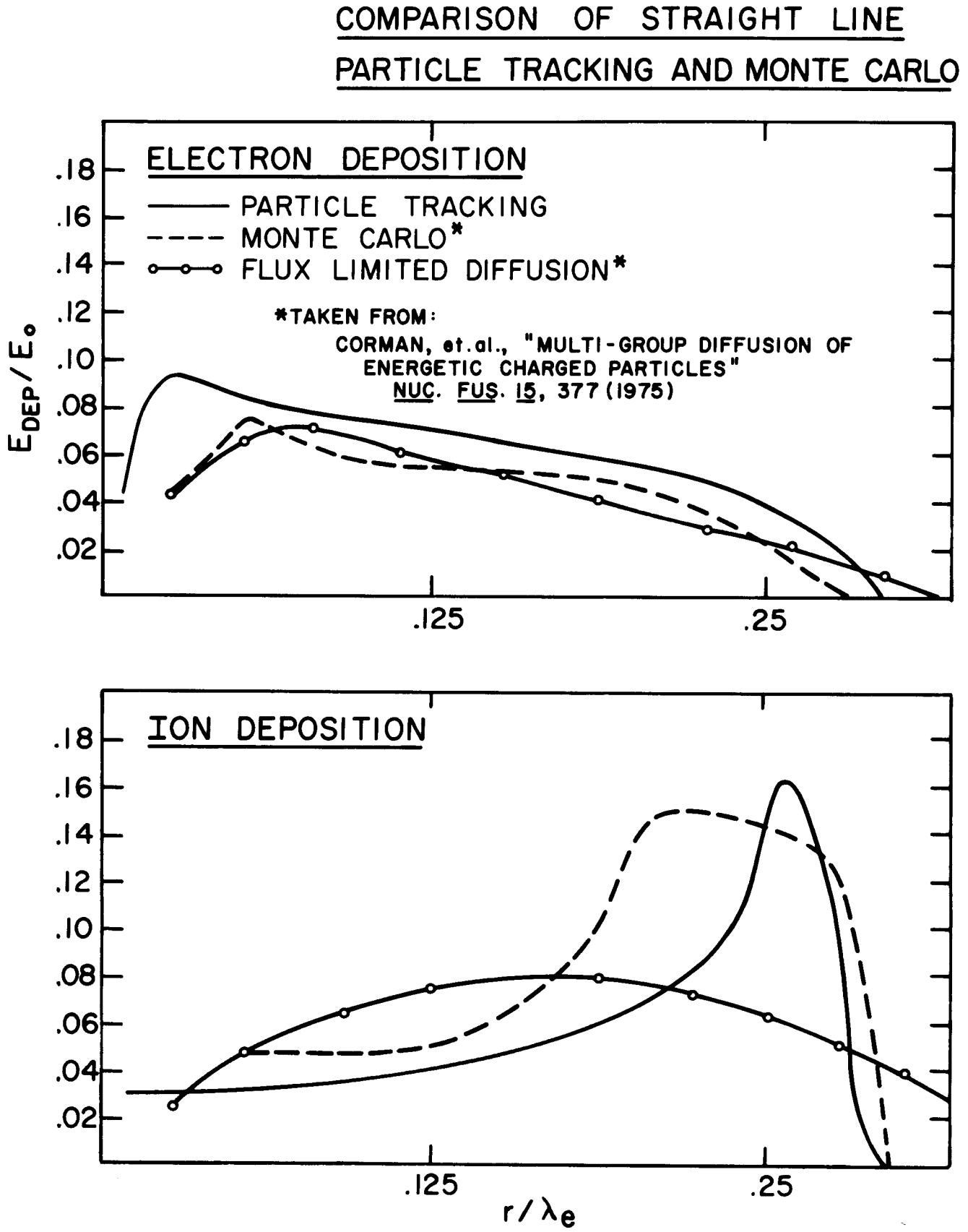
COMPARISON OF STRAIGHT LINE
PARTICLE TRACKING AND MONTE CARLO
ELECTRON DEPOSITION
PARTICLE TRACKING
MONTE CARLO*
FLUX LIMITED DIFFUSION*
*TAKEN FROM:
CORMAN, et.al., "MULTI-GROUP DIFFUSION OF ENERGETIC CHARGED PARTICLES"
NUC. FUS. 15, 377 (1975)
E_{DEP}/E_o
.18
.16
.14
.12
.10
.08
.06
.04
.02
.125
.25
ION DEPOSITION
r/λ_e

FIGURE 11

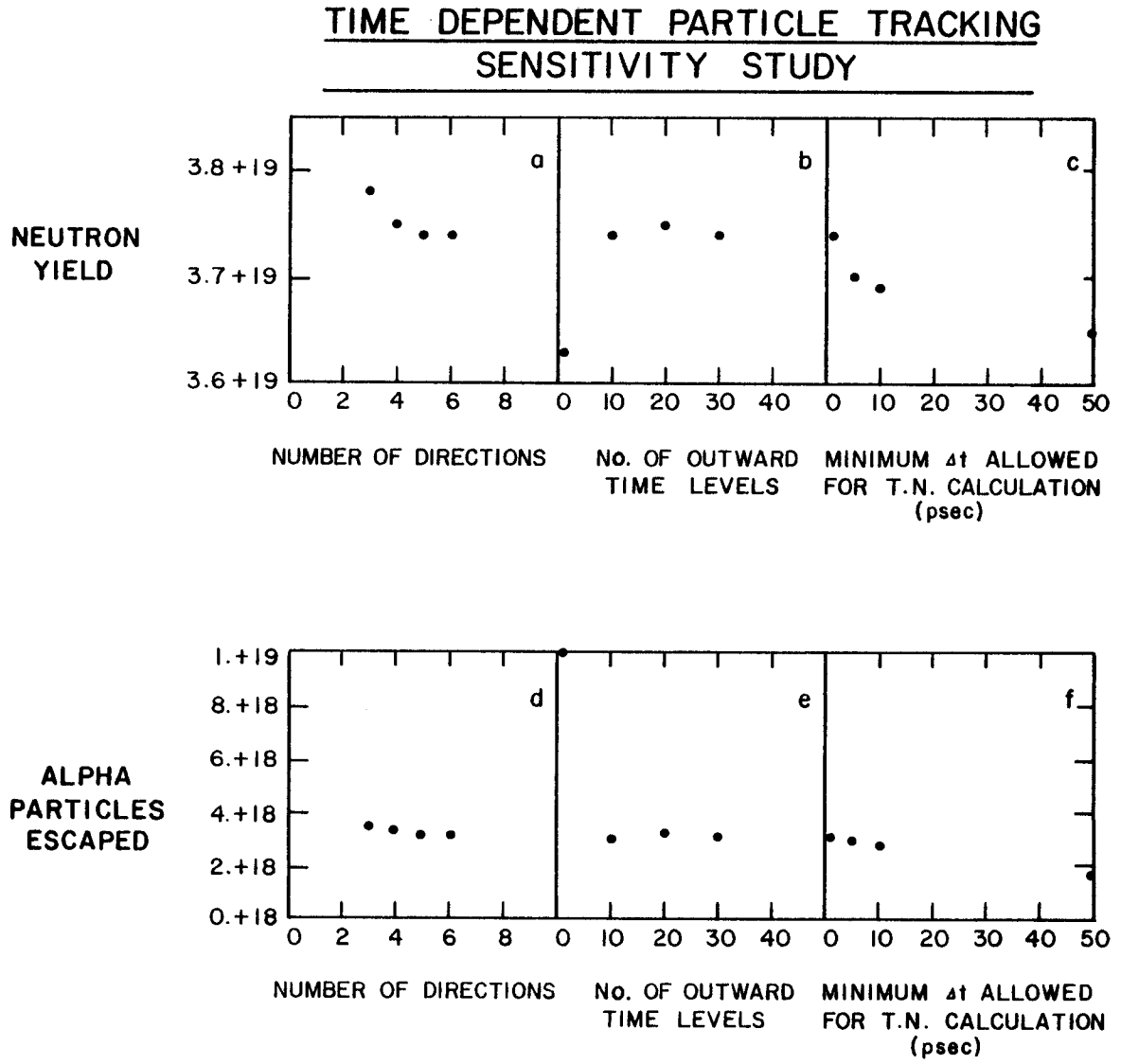
TIME DEPENDENT PARTICLE TRACKING
SENSITIVITY STUDY
NEUTRON YIELD
3.8+19
3.7+19
3.6+19
a
b
c
0 2 4 6 8
0 10 20 30 40
0 10 20 30 40 50
NUMBER OF DIRECTIONS
No. OF OUTWARD TIME LEVELS
MINIMUM Δt ALLOWED FOR T.N. CALCULATION (psec)
ALPHA PARTICLES ESCAPED
1.+19
8.+18
6.+18
4.+18
2.+18
0.+18
d
e
f
0 2 4 6 8
0 10 20 30 40
0 10 20 30 40 50
NUMBER OF DIRECTIONS
No. OF OUTWARD TIME LEVELS
MINIMUM Δt ALLOWED FOR T.N. CALCULATION (psec)

FIGURE 12

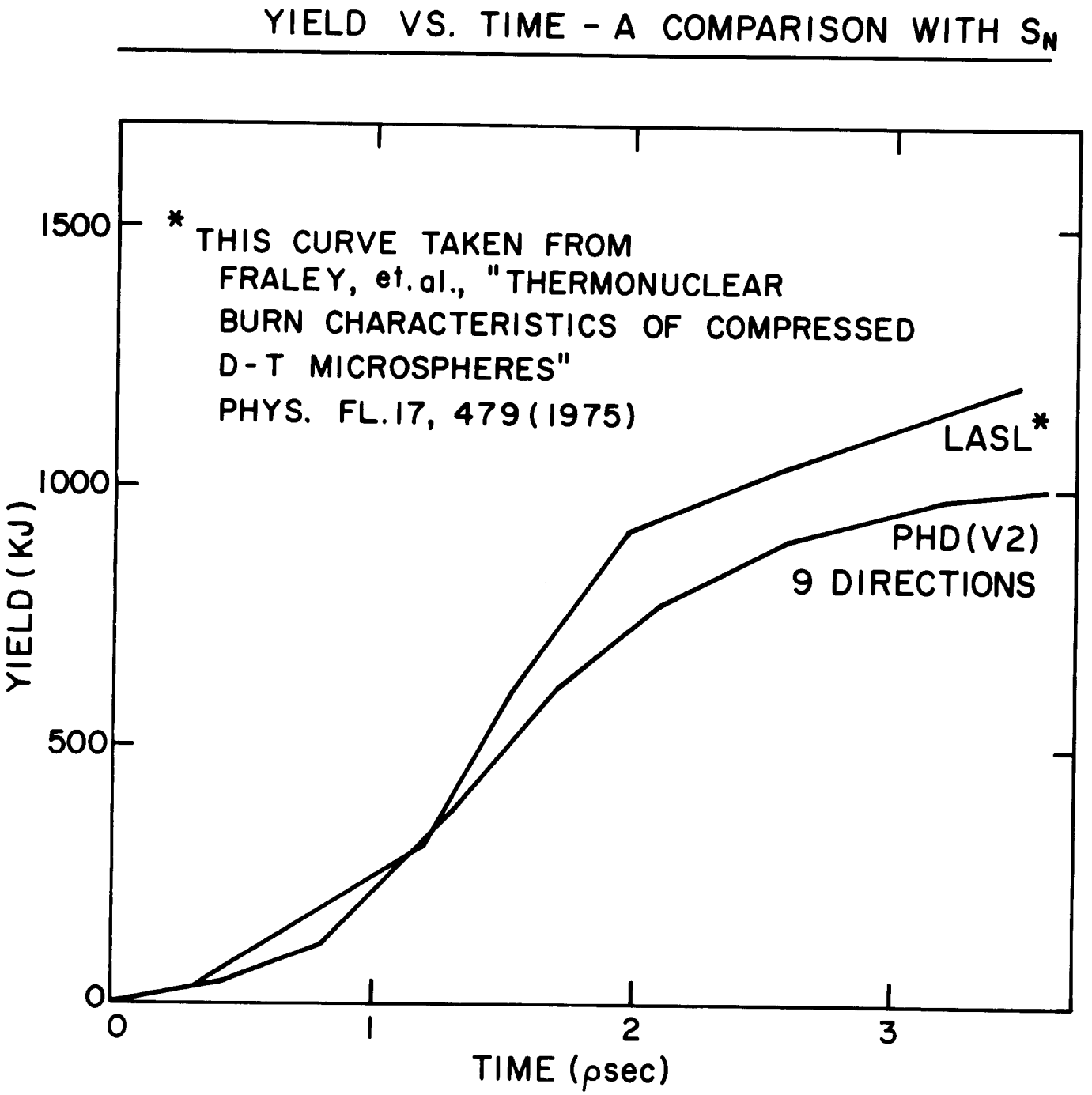
YIELD VS. TIME - A COMPARISON WITH S_N
* THIS CURVE TAKEN FROM FRALEY, et.al., "THERMONUCLEAR BURN CHARACTERISTICS OF COMPRESSED D-T MICROSPHERES" PHYS. FL.17, 479 (1975)
LASL*
PHD(V2) 9 DIRECTIONS
YIELD (KJ)
1500
1000
500
0
0
1
2
3
TIME (ρsec)

FIGURE 13